Stationary and dynamical properties of information entropies in nonextensive systems

Hideo Hasegawa*
Department of Physics, Tokyo Gakugei University, Koganei, Tokyo 184-8501, Japan
(Received 19 December 2007; revised manuscript received 21 January 2008; published 27 March 2008; publisher error corrected 1 April 2008)

The Tsallis entropy and Fisher information entropy (matrix) are very important quantities expressing information measures in nonextensive systems. Stationary and dynamical properties of the information entropies have been investigated in the N-unit coupled Langevin model subjected to additive and multiplicative white noise, which is one of typical nonextensive systems. We have made detailed, analytical and numerical study on the dependence of the stationary-state entropies on additive and multiplicative noise, external inputs, couplings, and number of constitutive elements (N). By solving the Fokker-Planck equation (FPE) by both the proposed analytical scheme and the partial difference equation method, transient responses of the information entropies to an input signal and an external force have been investigated. We have calculated the information entropies also with the use of the probability distribution derived by the maximum-entropy method, whose result is compared to that obtained by the FPE. The Cramér-Rao inequality is shown to be expressed by the extended Fisher entropy, which is different from the generalized Fisher entropy obtained from the generalized Kullback-Leibler divergence in conformity with the Tsallis entropy. The effect of additive and multiplicative colored noise on information entropies is discussed also.

DOI: 10.1103/PhysRevE.77.031133 PACS number(s): 05.70.−a, 05.10.Gg, 05.45.−a

I. INTRODUCTION

In the last one-half century, considerable studies have been made on the Boltzmann-Gibbs-Shannon entropy and the Fisher information entropy (matrix), both of which play important roles in thermodynamics and statistical mechanics of classical and quantum systems [1–7]. The entropy flux and entropy production have been investigated in connection with the space volume contraction [2]. In the information geometry [8], the Fisher information matrix provides us with the distance between the neighboring points in the Riemann space spanned by probability distributions. The Fisher information matrix gives the lower bound of estimation errors in the Cramér-Rao theorem. In a usual system consisting of N particles, the entropy and energy are proportional to N (extensive), and the probability distribution is given by the Gaussian distribution belonging to the exponential family.

In recent years, however, many efforts have been made for a study on nonextensive systems in which the physical quantity of N particles is not proportional to N [9–11]. The nonextensivity has been realized in various systems such as a system with long-range interactions, a small-scale system with large fluctuations in temperature and a multifractal system [11,12]. Tsallis has proposed the generalized entropy (called the Tsallis entropy hereafter) defined by [9,10]

$$S_q(t) = \frac{k}{(q-1)}\left(1 - \int p(x,t)^q dx\right) \tag{1}$$

$$= -k \int p(x,t)^q \ln_q p(x,t) dx, \tag{2}$$

where q is the entropic index, $p(x,t)$ denotes the probability distribution of a state x at time t, the Boltzmann constant k is hereafter unity, and $\ln_q x$ expresses the q-logarithmic function defined by $\ln_q x \equiv (1-x^{1-q})/(q-1)$. The Tsallis entropy accounts for the nonextensivity of the entropy in nonextensive systems. In the limit of $q \to 1$, $\ln_q x$ reduces to the normal $\ln x$ and then $S_q(t)$ agrees with the Boltzmann-Gibbs-Shannon entropy expressed by

$$S_1(t) = -\int p(x,t) \ln p(x,t) dx. \tag{3}$$

The probability distribution derived by the maximum-entropy method (MEM) with the use of the Tsallis entropy is given by non-Gaussian distribution [11], which reduces to the Gaussian and Cauchy distributions for $q=1$ and $q=2$, respectively.

Many authors have discussed the Fisher information matrix in nonextensive systems [13–24]. In order to derive the generalized Fisher information matrix $\mathbf{G}$ whose components are given by [19–24]

$$g_{ij} = g_{ji} = q \int p(x) \left(\frac{\partial \ln p(x)}{\partial \theta_i}\right)\left(\frac{\partial \ln p(x)}{\partial \theta_j}\right) dx, \tag{4}$$

the generalized Kullback-Leibler distance of $D(p|p')$ between the two distributions p and p' has been introduced,

$$D(p|p') = K(p|p') + K(p'|p), \tag{5}$$

with

$$K(p|p') = \int p(x)^q [\ln_q p(x) - \ln_q p'(x)] dx$$

$$= -\frac{1}{(q-1)}\left[1 - \int p(x)^q p'(x)^{1-q} dx\right], \tag{6}$$

where $p(x)=p(x;\{\theta_i\})$ and $\{\theta_i\}$ denotes a set of parameters specifying the distribution. In the limit of $q \to 1$, g_{ij} given by Eq. (4) reduces to the conventional Fisher information ma-

*hideohasegawa@goo.jp

trix. It should be remarked that Csiszár [25] had proposed the generalized divergence measure given by

$$D_C(p|p') = \int \left[p'(x) f\left(\frac{p(x)}{p'(x)} \right) + p(x) f\left(\frac{p'(x)}{p(x)} \right) \right] dx, \quad (7)$$

where $f(x)$ is assumed to be a convex function with the condition $f(1)=0$. For $f(p)=p \ln p$, Eq. (7) yields the conventional Kullback-Leibler divergence [26] given by

$$D_{\mathrm{KL}}(p|p') = \int \left[p(x) \ln\left(\frac{p(x)}{p'(x)} \right) + p'(x) \ln\left(\frac{p'(x)}{p(x)} \right) \right] dx. \quad (8)$$

Equation (7) for $f(p)=(q-1)^{-1}(p^q-p)$ leads to the generalized Kullback-Leibler distance given by Eqs. (5) and (6). The generalized divergence given by Eq. (6), which is in conformity with the Tsallis entropy, is equivalent to the α divergence of Amari [8] with $q=(1-\alpha)/2$ [27,28]. The escort probability and the generalized Fisher information matrix are discussed in Refs. [19,20]. The Fisher information entropy in the Cramér-Rao inequality has been studied for nonextensive systems [16,20,21].

Extensive studies on the Tsallis and Fisher entropies have been made for reaction-diffusion systems, by using the MEM with exact stationary and dynamical solutions for nonlinear FPE [13,14,17,18]. These studies nicely unify the concept of normal superdiffusion and subdiffusion by a single picture.

The purpose of the present paper is to investigate the stationary and dynamical properties of the information entropies in the coupled Langevin model which has been widely adopted for a study of various stochastic systems (for a recent review, see [29]). The Langevin model subjected to multiplicative noise is known to be one of typical nonextensive systems [11]. Recently the coupled Langevin model subjected to additive and multiplicative noise has been discussed with the use of the augmented moment method [30] which is the second-moment method for local and global variables [31,32]. We will obtain the probability distribution of the nonextensive, coupled Langevin model by using the Fokker-Planck equation (FPE) method with the mean-field approximation. We have made a detailed study on effects on the stationary information entropies of additive and multiplicative white noise, external force, input signal, couplings and the number of constituent elements in the adopted model. By solving the FPE both by the proposed analytical scheme and by the partial difference equation (PDE) method, we have investigated the transient responses to an input signal and an external force which are applied to the stationary state.

The outline of the paper is as follows. In Sec. II, we describe the adopted, N-unit coupled Langevin model. Analytical expressions for the Tsallis entropy and generalized Fisher information entropy in some limiting cases are presented. Numerical model calculations of stationary and dynamical entropies are reported. In Sec. III, discussions are presented on the entropy flux and entropy production and on a comparison between q-moment and normal-moment methods in which averages are taken over the escort and normal distributions, respectively. We will also discuss effects of additive and multiplicative colored noise on information entropies, by using the result recently obtained by the functional-integral method [33]. Section IV is devoted to our conclusion. In the Appendix, we summarize the information entropies calculated with the use of the probability distribution derived by the MEM. The Cramér-Rao inequality in nonextensive systems is shown to be expressed by the extended Fisher information entropy which is different from the generalized Fisher entropy.

II. COUPLED LANGEVIN MODEL

A. Adopted model

We have adopted the N-unit coupled Langevin model subjected to additive and multiplicative white noise given by

$$\frac{dx_i}{dt} = F(x_i) + \beta \xi_i(t) + \alpha G(x_i)\eta_i(t) + I_i(t), \quad (9)$$

with

$$I_i(t) = \frac{J}{(N-1)} \sum_{j(\neq i)} [x_j(t) - x_i(t)] + I(t) \quad (i = 1 \text{ to } N). \quad (10)$$

Here $F(x)$ and $G(x)$ denote arbitrary functions of x, J the coupling strength, $I(t)$ an external input, α and β are the strengths of multiplicative and additive noise, respectively, and $\eta_i(t)$ and $\xi_i(t)$ express zero-mean Gaussian white noises with correlations given by

$$\langle \eta_i(t)\eta_j(t') \rangle = \delta_{ij}\delta(t-t'), \quad (11)$$

$$\langle \xi_i(t)\xi_j(t') \rangle = \delta_{ij}\delta(t-t'), \quad (12)$$

$$\langle \eta_i(t)\xi_j(t') \rangle = 0. \quad (13)$$

We have adopted the mean-field approximation for $I_i(t)$ given by

$$I_i(t) \simeq \hat{J}[\mu_q(t) - x_i(t)] + I(t), \quad (14)$$

with

$$\hat{J} = \frac{JN}{(N-1)}, \quad (15)$$

$$\mu_q(t) = \frac{1}{N} \sum_i E_q[x_i(t)], \quad (16)$$

where the $E_q[\cdots]$ expresses the average over the escort distribution to be shown below [Eqs. (20)–(22)].

B. Fokker-Planck equation

Owing to the adopted mean-field approximation given by Eq. (14), each element of the ensemble is ostensibly independent. The total probability distribution of $p(\{x_k\},t)$ is given by the product of that of each element,

$$p(\{x_k\},t) = \Pi_i p_i(x_i,t), \quad (17)$$

where the FPE for $p_i(x_i,t)$ in the Stratonovich representation is given by

$$\frac{\partial}{\partial t}p_i(x_i,t) = -\frac{\partial}{\partial x_i}[F(x_i)+I_i(t)]p_i(x_i,t) + \left(\frac{\beta^2}{2}\right)\frac{\partial^2}{\partial x_i^2}p_i(x_i,t) + \left(\frac{\alpha^2}{2}\right)\frac{\partial}{\partial x_i}G(x_i)\frac{\partial}{\partial x_i}G(x_i)p_i(x_i,t). \quad (18)$$

The expectation value of $\mu_q(t)$ is given by

$$\mu_q(t) = E_q[x_i(t)], \quad (19)$$

with

$$E_q[x_i(t)^m] = \int P_{iq}(x_i,t)x_i^m dx_i \quad (m=1,2), \quad (20)$$

where the escort probability distribution $P_{iq}(x_i,t)$ is given by

$$P_{iq}(x_i,t) = \frac{1}{c_{iq}(t)}p_i(x_i,t)^q, \quad (21)$$

$$c_{iq}(t) = \int p_i(x_i,t)^q dx_i. \quad (22)$$

It is noted that $\mu_q(t)$ and $p_i(x_i,t)$ are self-consistently determined from Eqs. (14) and (18). The relevant fluctuation (variance) of $\sigma_q(t)^2$ is given by

$$\sigma_q(t)^2 = E_q[(x_i-\mu_q)^2]. \quad (23)$$

When we adopt $F(x)$ and $G(x)$ given by

$$F(x) = -\lambda x, \quad (24)$$

$$G(x) = x, \quad (25)$$

where λ denotes the relaxation rate, the FPE for $p(x,t)$ is expressed by (the subscript i is hereafter neglected)

$$\frac{\partial}{\partial t}p(x,t) = \left(\lambda+\hat{J}+\frac{\alpha^2}{2}\right)p(x,t) + \left[\left(\lambda+\hat{J}+\frac{3\alpha^2}{2}\right)x - u(t)\right]\frac{\partial}{\partial x}p(x,t) + \left(\frac{\alpha^2}{2}x^2+\frac{\beta^2}{2}\right)\frac{\partial^2}{\partial x^2}p(x,t), \quad (26)$$

with

$$u(t) = \hat{J}\mu_q(t) + I(t). \quad (27)$$

From the FPE given by Eq. (26), the stationary distribution is given by [30,34,35]

$$\ln p(x) \propto -\left(\frac{2\lambda+2\hat{J}+\alpha^2}{2\alpha^2}\right)\ln(\alpha^2x^2+\beta^2) + Y(x) \quad (28)$$

$$\propto -\left(\frac{1}{q-1}\right)\ln\left[1+(q-1)\left(\frac{x^2}{2\phi^2}\right)\right] + Y(x), \quad (29)$$

with

$$q = 1+\frac{2\alpha^2}{(2\lambda+2\hat{J}+\alpha^2)}, \quad (30)$$

$$\phi^2 = \frac{\beta^2}{(2\lambda+2\hat{J}+\alpha^2)}, \quad (31)$$

$$Y(x) = \left(\frac{2u}{\alpha\beta}\right)\tan^{-1}\left(\frac{\alpha x}{\beta}\right), \quad (32)$$

$$u = \hat{J}\mu_q + I, \quad (33)$$

where the entropic index is given for $1 \le q < 3$. Equation (29) yields the q-Gaussian distribution given by

$$p(x) = \frac{1}{Z_q}\exp_q\left(-\frac{x^2}{2\phi^2}\right)e^{Y(x)}, \quad (34)$$

with

$$Z_q = \int \exp_q\left(-\frac{x^2}{2\phi^2}\right)e^{Y(x)}dx, \quad (35)$$

where $\exp_q(x)$ stands for the q-exponential function defined by $\exp_q(x) \equiv [1+(1-q)x]_+^{1/(1-q)}$, where $[y]_+ = y$ for $y \ge 0$ and 0 for $y < 0$.

Some limiting cases of Eq. (34) are examined in the following.

(1) For $\alpha = 0$ and $\beta \neq 0$ (i.e., additive noise only),

$$p(x) = \frac{1}{\sqrt{2\pi\sigma_1^2}}e^{-(1/2\sigma_1^2)(x-\mu_1)^2}, \quad (36)$$

which yield

$$\mu_1 = \frac{2\phi^2 u}{\beta^2} = \frac{u}{(\lambda+\hat{J})}, \quad (37)$$

$$\sigma_1^2 = \phi^2 = \frac{\beta^2}{2(\lambda+\hat{J})}. \quad (38)$$

(2) For $\alpha \neq 0$, $\beta = 0$ (i.e., multiplicative noise only) [30,34,35],

$$p(x) = \frac{1}{Z_q}|x|^{-\delta}e^{-\kappa/x}\Theta(x/\kappa) \quad \text{for } u \neq 0, \quad (39)$$

$$\propto |x|^{-\delta} \quad \text{for } u = 0, \quad (40)$$

with

$$Z_q = \frac{\Gamma(\delta-1)}{\kappa^{\delta-1}} = \frac{\Gamma[(3-q)/(q-1)]}{\kappa^{(3-q)/(q-1)}} \quad \text{for } u \neq 0, \quad (41)$$

$$\delta = \frac{2}{(q-1)}, \quad (42)$$

$$\kappa = \frac{2u}{\alpha^2} = \frac{2(\hat{J}\mu_q+I)}{\alpha^2}, \quad (43)$$

where $\Gamma(x)$ and $\Theta(x)$ denote the Γ and Heaviside functions, respectively, and Z_q diverges for $u=0$. For $u \neq 0$, Eqs. (39) and (41) yield

$$\mu_q = \frac{q(q-1)}{2}\kappa, \tag{44}$$

$$\sigma_q^2 = \frac{q^2(q-1)^3}{4(3-q)}\kappa^2. \tag{45}$$

The distribution given by Eq. (39) has a peak at $x=\kappa/\delta = \mu_q/q$.

(3) For $\alpha \neq 0$, $\beta \neq 0$, $u=\hat{J}\mu_q+I=0$ (i.e., without coupling and external input) [30,34,35],

$$p(x) = \frac{1}{Z_q}\exp_q\left(-\frac{x^2}{2\phi^2}\right), \tag{46}$$

$$Z_q = \left(\frac{2\phi^2}{q-1}\right)^{1/2} B\left(\frac{1}{2}, \frac{1}{q-1}-\frac{1}{2}\right), \tag{47}$$

which lead to

$$\mu_q = 0, \tag{48}$$

$$\sigma_q^2 = \frac{2\phi^2}{(3-q)} = \frac{\beta^2}{2\lambda}. \tag{49}$$

It is noted that when we adopt normal moments averaged over the q-Gaussian given by

$$E[x(t)^m] = \int p(x,t)x(t)^m dx, \tag{50}$$

instead of the q moments given by Eq. (20), its stationary variance is given by $\sigma^2 = E[(x-E[x])^2] = \beta^2/2(\lambda-\alpha^2)$ which diverges at $\lambda=\alpha^2$ [30].

C. Tsallis entropy

With the use of the total distribution of $p(\{x_i\})$ given by Eq. (17), the Tsallis entropies of single-unit and N-unit ensembles are given by

$$S_q^{(1)} = \left(\frac{1-c_q}{q-1}\right), \tag{51}$$

$$S_q^{(N)} = \left(\frac{1-\Pi_i c_{iq}}{q-1}\right) = \left(\frac{1-c_q^N}{q-1}\right), \tag{52}$$

with

$$c_q = c_{iq} = \int p_i(x_i)^q dx_i. \tag{53}$$

Eliminating c_q from Eqs. (51) and (52), we get

$$S_q^{(N)} = \sum_{k=1}^{N} C_k^N (-1)^{k-1}(q-1)^{k-1}(S_q^{(1)})^k \tag{54}$$

$$= NS_q^{(1)} - \frac{N(N-1)}{2}(q-1)(S_q^{(1)})^2 + \cdots, \tag{55}$$

where $C_k^N = N!/(N-k)!k!$. Equation (54) shows that the Tsallis entropy is non-extensive except for $q=1.0$, for which $S_q^{(N)}$ reduces to the extensive Boltzmann-Gibbs-Shannon entropy, $S_1^{(N)} = NS_1^{(1)}$.

Substituting the stationary distributions given by Eqs. (36), (39), and (46) to Eq. (1), we obtain the analytic expression for the Tsallis entropy of a single unit given by

$$S_q^{(1)} = \left(\frac{1}{2}\right)[1+\ln(2\pi\sigma_q^2)] \quad \text{for} \quad \alpha=0, \quad \beta\neq 0, \tag{56}$$

$$= \left(\frac{1-c_q}{q-1}\right) \quad \text{for} \quad \alpha \neq 0, \tag{57}$$

with

$$c_q = \frac{1}{Z_q^q}\frac{\Gamma(q\delta-1)}{(q\kappa)^{q\delta-1}} = \frac{1}{Z_q^q}\frac{\Gamma[(q+1)/(q-1)]}{(q\kappa)^{(q+1)/(q-1)}} \tag{58}$$

$$\text{for} \quad \alpha \neq 0, \quad \beta = 0, \quad u \neq 0,$$

$$= \frac{1}{Z_q^q}\left(\frac{2\phi^2}{q-1}\right)^{1/2} B\left(\frac{1}{2}, \frac{q}{q-1}-\frac{1}{2}\right) = \left(\frac{3-q}{2}\right)Z_q^{1-q} \tag{59}$$

$$\text{for} \quad \alpha \neq 0, \quad \beta \neq 0, \quad u = 0,$$

where $B(a,b)$ stands for the β function, and Z_q in Eqs. (58) and (59) are given by Eqs. (41) and (47), respectively.

D. Generalized Fisher information entropy

We consider the generalized Fisher information entropy given by

$$g_q = q\int p(x)\left(\frac{\partial \ln p(x)}{\partial\theta}\right)^2 dx. \tag{60}$$

From Eqs. (17) and (60), the generalized Fisher entropy for the N-unit system is given by

$$g_q^{(N)} = qE\left[\left(\frac{\partial \ln p(x)}{\partial\theta}\right)^2\right] \tag{61}$$

$$= q\int\cdots\int\left(\sum_i \frac{\partial \ln p_i(x_i)}{\partial\theta}\right)^2 \Pi_i p_i(x_i)dx_i \tag{62}$$

$$= q\sum_i \int\left(\frac{\partial \ln p_i(x_i)}{\partial\theta}\right)^2 p_i(x_i)dx_i + \Delta g_q \tag{63}$$

$$= Ng_q^{(1)}, \tag{64}$$

because the cross term Δg_q of Eq. (63) vanishes,

$$\Delta g_q = q\sum_{i(\neq j)}\sum_j \int\left(\frac{\partial \ln p_i(x_i)}{\partial\theta}\right)p_i(x_i)dx_i\int\left(\frac{\partial \ln p_j(x_j)}{\partial\theta}\right) \times p_j(x_j)dx_j \tag{65}$$

$$= q\sum_{i(\neq j)}\sum_j \int\frac{\partial p_i(x_i)}{\partial\theta}dx_i\int\frac{\partial p_j(x_j)}{\partial\theta}dx_j \tag{66}$$

$$= q \sum_{i(\neq j)} \sum_{j} \frac{\partial}{\partial \theta} \int p_i(x_i) dx_i \frac{\partial}{\partial \theta} \int p_j(x_j) dx_j \tag{67}$$

$$= 0, \tag{68}$$

where $g_q^{(1)}$ stands for the generalized Fisher entropy in a single subsystem. The generalized Fisher information entropy is extensive in the nonextensive system as shown in [27],

$$g_q^{(N)} = N g_q^{(1)}. \tag{69}$$

The probability distribution $p(x)$ obtained by the FPE for our Langevin model is determined by the six parameters of λ, α, β, J, I, and N. When we adopt $\theta = I$ in Eq. (60), for example, we obtain the generalized Fisher entropy given by

$$g_q = q \left\{ E\left[\left(\frac{\partial Y(x)}{\partial I} \right)^2 \right] - E\left[\left(\frac{\partial Y(x)}{\partial I} \right) \right]^2 \right\}, \tag{70}$$

where $E[\cdots]$ expresses the average over $p(x)$ [Eq. (50)].

Alternatively we have adopted the generalized Fisher entropy given by

$$g_q = q \int p(x) \left(\frac{\partial \ln p(x)}{\partial x} \right)^2 dx, \tag{71}$$

which is obtainable for g_q with $\theta = \mu_q$ in Eq. (60) if $p(x)$ is given by the MEM [Eqs. (102) and (A10)]. Although $p(x)$ derived by the FPE is not explicitly specified by μ_q and σ_q^2, we have employed Eq. (71) in our following discussion, expecting it is meaningful for both cases of the FPE and MEM. Substituting the stationary distributions given by Eqs. (36), (39), and (46) to Eq. (71), we obtain the analytic expression for the generalized Fisher entropy for $N=1$ given by

$$g_q^{(1)} = \left(\frac{1}{\sigma_1^2} \right) = \frac{2(\lambda + \hat{J})}{\beta^2} \quad \text{for} \quad \alpha = 0, \quad \beta \neq 0, \tag{72}$$

$$= \left(\frac{q}{\kappa^2} \right) \delta(\delta - 1)(\delta + 2) = \frac{q^4}{\sigma_q^2} \quad \text{for} \quad \alpha \neq 0, \quad \beta = 0, \quad u \neq 0, \tag{73}$$

$$= \left(\frac{2q}{(q-1)\phi^2} \right) \frac{B\left(\frac{3}{2}, \frac{1}{q-1} + \frac{1}{2}\right)}{B\left(\frac{1}{2}, \frac{1}{q-1} - \frac{1}{2}\right)} = \frac{1}{\sigma_q^2}$$

$$\text{for} \quad \alpha \neq 0, \quad \beta \neq 0, \quad u = 0, \tag{74}$$

where σ_q^2 in Eqs. (73) and (74) are given by Eqs. (45) and (49), respectively.

E. Stationary properties

1. Calculation method

The adopted Langevin model includes six parameters of λ, α, β, J, I, and N. The dependence of the Tsallis entropy and generalized Fisher information entropy on these parameters has been studied by numerical methods. We have calculated the distribution $p(x)$ by the FPE [Eqs. (34) and (35)], and also by direct simulations (DSs) for the Langevin model [Eqs. (9) and (10)] with the Heun method: DS results are averages of 100 trials.

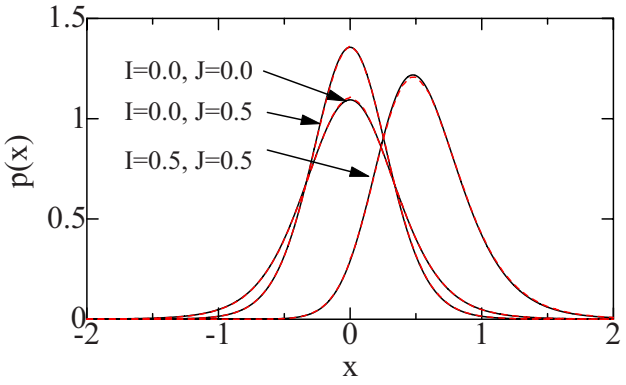

FIG. 1. (Color online) Stationary distribution $p(x)$ for $(I,J) = (0.0,0.0)$, $(0.0,0.5)$, and $(0.5,0.5)$ with $\lambda = 1.0$, $\alpha = 0.5$, and $\beta = 0.5$, calculated by the FPE [Eqs. (34) and (35)] (solid curves) and by DSs for the coupled Langevin model [Eqs. (9) and (10)] (dashed curves), results of FPE and DSs being indistinguishable.

2. Model calculations

Figures 1(a)–1(c) show three examples of the stationary distribution $p(x)$ for $(I,J) = (0.0,0.0)$, $(0.0,0.5)$, and $(0.5,0.5)$ with $\lambda = 1.0$, $\alpha = 0.5$, $\beta = 0.5$, and $N = 100$. Solid curves show the results calculated with the use of the FPE whereas dashed curves show those of DSs for the Langevin equation: Both results are in good agreement and indistinguishable. When the coupling strength is increased from $J = 0.0$ to $J = 0.5$ with $I = 0.0$, the width of $p(x)$ is decreased because of a decreased ϕ^2 in Eq. (31). When an input of $I = 0.5$ is applied, $p(x)$ changes its position by an amount of about 0.5 with a slight variation of its shape: $p(x)$ for $(I,J) = (0.5,0.5)$ is not a simple translational shift of $p(x)$ for $(I,J) = (0.0,0.5)$.

In the following, we will discuss model calculations of the dependence on α, β, I, J, and N, whose results are shown in Figs. 2–6, respectively [dotted curves in the frames (a) and (b) in Figs. 2–5 will be explained in Sec. III C].

α dependence. First we show μ_q, σ_q^2, S_q, and g_q in Figs. 2(a)–2(d), respectively, plotted as a function of α^2 for $I = 0.0$ (chain curves), $I = 0.5$ (dashed curves), and $I = 1.0$ (solid curves) with $\lambda = 1.0$, $\beta = 0.5$, and $J = 0.0$. Figure 2(a) shows that the α dependence of μ_q is very weak. We note in Fig. 2(b) that for $I = 0.5$ and $I = 1.0$, σ_q^2 is linearly increased with increasing α^2 though σ_q^2 is independent of α for $I = 0.0$. Figure 2(c) shows that with increasing α^2, S_q is increased with broad maxima at $\alpha^2 \sim 0.8$ for $I = 1.0$ and at $\alpha^2 \sim 1.5$ for $I = 0.5$. With increasing α^2 from $\alpha^2 = 0$, in contrast, g_q is decreased for $I = 0.5$ and $I = 1.0$ with broad minima, whereas g_q is independent of α^2 for $I = 0.0$. For larger I, S_q, and g_q have stronger α^2 dependence.

β dependence. Figures 3(a)–3(d) show μ_q, σ_q^2, S_q, and g_q, respectively, plotted as a function of β^2 for $I = 0.0$ (chain curves), $I = 0.5$ (dashed curves), and $I = 1.0$ (solid curves) with $\lambda = 1.0$, $\alpha = 0.5$, and $J = 0.0$. With increasing β, μ_q has no changes although σ_q^2 is linearly increased. With increasing β^2

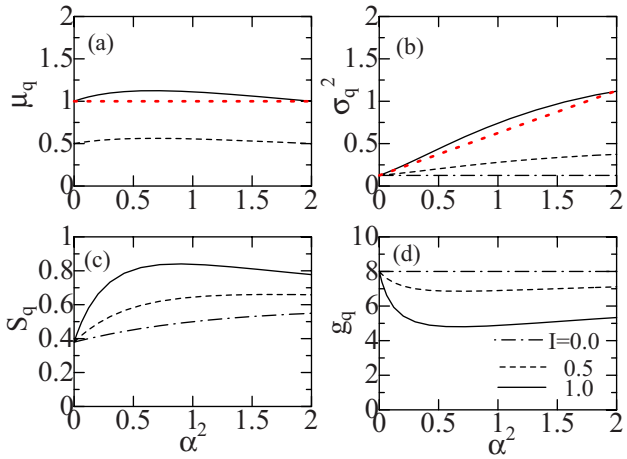

FIG. 2. (Color online) The α^2 dependence of (a) μ_q, (b) σ_q^2, (c) S_q, and (d) g_q for $I=0.0$ (chain curves), $I=0.5$ (dashed curves), and $I=1.0$ (solid curves) with $\lambda=1.0$, $\beta=0.5$, and $J=0.0$. Dotted curves in (a) and (b) express the analytical result given by Eqs. (84) and (85) for $I=1.0$.

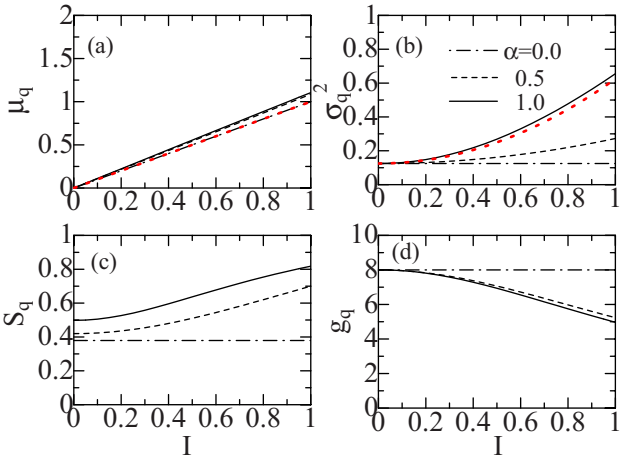

FIG. 4. (Color online) The I dependence of (a) μ_q, (b) σ_q^2, (c) S_q, and (d) g_q for $\alpha=0.0$ (chain curves), $\alpha=0.5$ (dashed curves), and $\alpha=1.0$ (solid curves) with $\lambda=1.0$, $\beta=0.5$, and $J=0.0$. Dotted curves in (a) and (b) express the analytical result given by Eqs. (84) and (85) for $\alpha=1.0$.

from $\beta^2=0.0$, S_q (g_q) is significantly increased (decreased). This trend is more significant for $I=0.0$ than for $I=0.5$ and $I=1.0$.

I dependence. The I dependence of μ_q, σ_q^2, S_q, and g_q are shown in Figs. 4(a)–4(d) for $\alpha=0.0$ (chain curves), $\alpha=0.5$ (dashed curves), and $\alpha=1.0$ (solid curves) with $\lambda=1.0$. The gradient of μ_q versus I is slightly larger for larger α. In the case of $\alpha=0.0$, σ_q^2, S_q, and g_q are independent of I [see Eqs. (56) and (72)]. With increasing I for finite α, S_q is increased while g_q is decreased.

J dependence. We show the J dependence of μ_q, σ_q^2, S_q, and g_q in Figs. 5(a)–5(d), for $I=0.0$ (chain curves), $I=0.5$ (dashed curves), and $I=1.0$ (solid curves) with $\lambda=1.0$, $\alpha=0.5$, $\beta=0.5$, and $N=100$. We note that μ_q is independent of J. With increasing J, σ_q^2 and S_q are linearly decreased whereas g_q is increased.

N dependence. Figure 6 shows the Tsallis entropy per element, $S_q^{(N)}/N$, given by [Eq. (55)]

$$\frac{S_q^{(N)}}{N} = S_q^{(1)} - \frac{1}{2}(N-1)(q-1)(S_q^{(1)})^2 + \cdots \tag{75}$$

for $\alpha=0.0$ (dotted curve), $\alpha=0.1$ (solid curve), $\alpha=0.5$ (dashed curve), and $\alpha=1.0$ (chain curve) with $\lambda=1.0$, $\beta=0.5$, $I=0.0$, and $J=0.0$. Note that for $\alpha=0.0$ ($q=1.0$), the system is extensive because $S_1^{(N)}/N=S_1^{(1)}$. For finite α, however, it is nonextensive: $S_q^{(N)}/N$ is more significantly de-

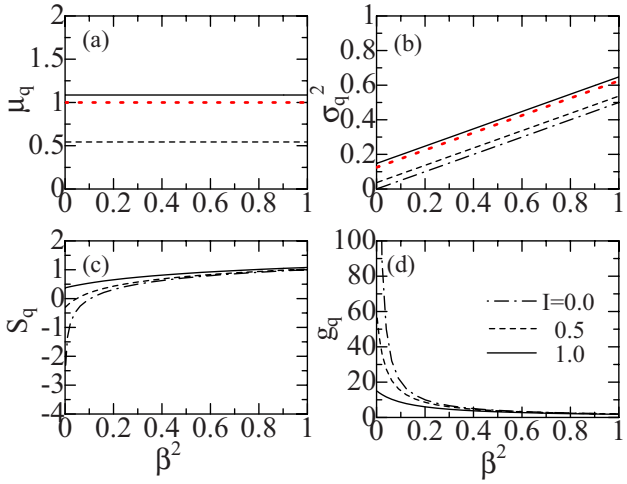

FIG. 3. (Color online) The β^2 dependence of (a) μ_q, (b) σ_q^2, (c) S_q, and (d) g_q for $I=0.0$ (chain curves), $I=0.5$ (dashed curves), and $I=1.0$ (solid curves) with $\lambda=1.0$, $\alpha=0.5$, and $J=0.0$. Dotted curves in (a) and (b) express the analytical result given by Eqs. (84) and (85) for $I=1.0$.

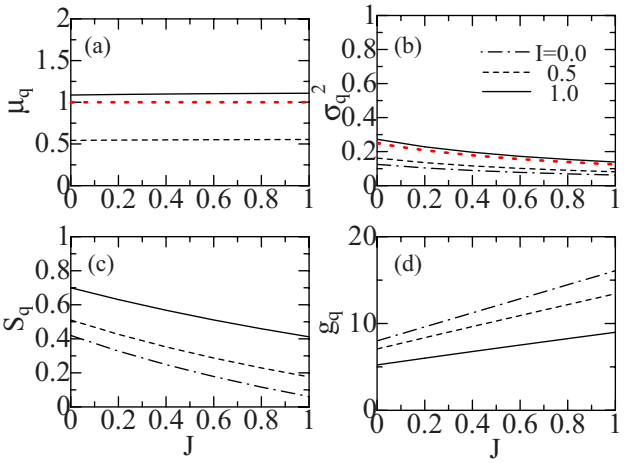

FIG. 5. (Color online) The J dependence of (a) μ_q, (b) σ_q^2, (c) S_q, and (d) g_q for $I=0.0$ (chain curves), $I=0.5$ (dashed curves), and $I=1.0$ (solid curves) with $\lambda=1.0$, $\alpha=0.5$, $\beta=0.5$, and $N=100$. Dotted curves in (a) and (b) express the analytical result given by Eqs. (84) and (85) for $I=1.0$.

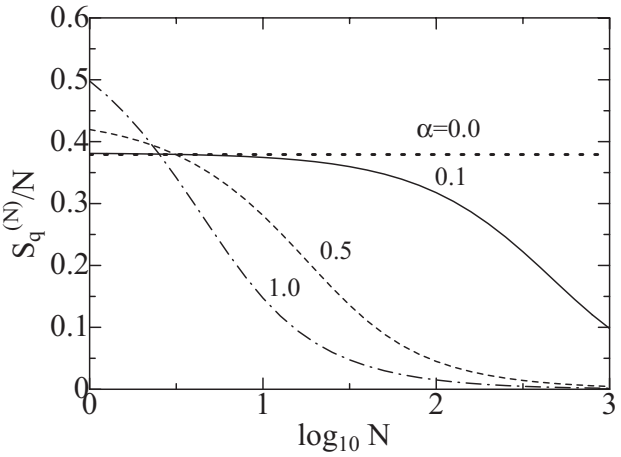

FIG. 6. The N dependence of the Tsallis entropy per element, $S_q^{(N)}/N$, for $\alpha=0.0$ (dotted curve), $\alpha=0.1$ (solid curve), $\alpha=0.5$ (dashed curve), and $\alpha=1.0$ (chain curve) with $\lambda=1.0$, $\beta=0.5$, $I=0.0$, and $J=0.0$.

creased for larger α, though the generalized Fisher information entropy g_q is extensive [Eq. (69)].

F. Dynamical properties

1. Analytical method for the FPE

In order to discuss the dynamical properties of the entropies, we must calculate the time-dependent probability $p(x,t)$, solving the FPE given by Eq. (26). In the case of $q=1.0$, we may obtain the exact solution of the Gaussian distribution given by

$$p(x,t) = \frac{1}{\sqrt{2\pi\sigma_1(t)^2}} e^{-[x-\mu_1(t)]^2/2\sigma_1(t)^2}, \tag{76}$$

where $\mu_1(t)$ and $\sigma_1(t)^2$ satisfy equations of motion given by

$$\frac{d\mu_1(t)}{dt} = -\lambda\mu_1(t) + I, \tag{77}$$

$$\frac{d\sigma_1(t)^2}{dt} = -2(\lambda+\hat{J})\sigma_1(t)^2 + \beta^2. \tag{78}$$

In order to obtain an analytical solution of the FPE for $q>1.0$, we have adopted the following method.

(1) Starting from an equation of motion for the nth q moment of $E_q[x^n]$ given by

$$\frac{dE_q[x^n]}{dt} = \frac{d}{dt}\int P_q(x,t)x^n dx \tag{79}$$

$$= \frac{q}{c_q}\int \left(\frac{\partial p(x,t)}{\partial t}\right) p(x,t)^{q-1} x^n dx - \frac{1}{c_q}\left(\frac{dc_q}{dt}\right) E_q[x^n], \tag{80}$$

$$\frac{dc_q}{dt} = q\int \left(\frac{\partial p(x,t)}{\partial t}\right) p(x,t)^{q-1} dx, \tag{81}$$

we have obtained equations of motion for $\mu_q(t)$ $(=E_q[x])$ and $\sigma_q(t)^2$ $(=E_q[x^2]-E[x]^2)$, valid for $O(\alpha^2)$ and $O(\beta^2)$, as given by [30]

$$\frac{d\mu_q(t)}{dt} \simeq -\lambda\mu_q(t) + I, \tag{82}$$

$$\frac{d\sigma_q(t)^2}{dt} \simeq -2(\lambda+\hat{J})\sigma_q(t)^2 + \alpha^2\mu_q(t)^2 + \beta^2. \tag{83}$$

Equations (82) and (83) lead to the stationary solution given by

$$\mu_q = \frac{I}{\lambda}, \tag{84}$$

$$\sigma_q^2 = \frac{(\alpha^2\mu_q^2+\beta^2)}{2(\lambda+\hat{J})} = \frac{(\alpha^2 I^2/\lambda^2+\beta^2)}{2(\lambda+\hat{J})}. \tag{85}$$

(2) We rewrite the distribution of $p(x)$ given by Eqs. (30)–(35) in terms of μ_q, σ_q^2 and q, as

$$p(x) = \frac{1}{Z_q}\left[1-(1-q)\left(\frac{x^2}{2\phi^2}\right)\right]^{1/(1-q)} e^{Y(x)}, \tag{86}$$

with

$$Y(x) = \left(\frac{(3-q)\mu_q}{\sqrt{2(q-1)\phi^2}}\right)\tan^{-1}\left(\sqrt{\frac{(q-1)}{2\phi^2}}x\right), \tag{87}$$

$$\phi^2 = \left(\frac{3-q}{2}\right)\sigma_q^2 - \left(\frac{q-1}{2}\right)\mu_q^2, \tag{88}$$

where Z_q expresses the normalization factor [Eq. (35)]. In deriving Eqs. (86)–(88), we have employed relations given by

$$\alpha^2 = \frac{2(q-1)(\lambda+\hat{J})}{(3-q)}, \tag{89}$$

$$\beta^2 = 2(\lambda+\hat{J})\left(\sigma_q^2 - \frac{(q-1)\mu_q^2}{(3-q)}\right), \tag{90}$$

which are obtained from Eqs. (30), (84), and (85).

(3) Then we have assumed that a solution of $p(x,t)$ of the FPE given by Eq. (26) is expressed by Eqs. (86)–(88) in which stationary μ_q and σ_q^2 are replaced by time-dependent $\mu_q(t)$ and $\sigma_q(t)^2$ with equations of motion given by Eqs. (82) and (83).

Dotted curves in the frames (a) and (b) of Figs. 3–6 express the results of stationary μ_q and σ_q^2 calculated by Eqs. (84) and (85) for some typical sets of parameters. They are in good agreement with those shown by solid curves obtained with the use of the stationary distribution of $p(x)$ given by Eq. (34).

As we will show, the approximate, analytical method given by Eqs. (82), (83), and (86)–(88) provides fairly good

results for dynamics of $\mu_q(t)$, $\sigma_q(t)^2$, and $S_q(t)$, and also for that of $g_q(t)$ except for the transient period.

2. Partial difference equation method

In order to examine the validity of the analytical method discussed above, we have adopted also the numerical method, using the PDE derived from Eq. (26), as given by

$$p(x,t+b) = p(x,t) + \left(\lambda + \hat{J} + \frac{\alpha^2}{2}\right)bp(x,t) + \left[x\left(\lambda + \hat{J} + \frac{3\alpha^2}{2}\right) - u(t)\right]\left(\frac{b}{2a}\right)[p(x+a) - p(x-a)] + \left(\frac{\alpha^2}{2}x^2 + \frac{\beta^2}{2}\right) \times \left(\frac{b}{a^2}\right)[p(x+a,t) + p(x-a,t) - 2p(x,t)], \quad (91)$$

with

$$u(t) = \hat{J}\mu_q(t) + I(t), \quad (92)$$

where a and b denote incremental steps of x and t, respectively.

We impose the boundary condition

$$p(x,t) = 0 \quad \text{for} \quad |x| \geq x_m, \quad (93)$$

with $x_m=5$, and the initial condition of $p(x,0)=p_0(x)$, where $p_0(x)$ is the stationary distribution given by Eqs. (34) and (35). We have chosen parameters of $a=0.05$ and $b=0.0001$ such as to satisfy the condition $(\alpha^2 x_m^2 b/2a^2) < 1/2$, which is required for stable, convergent solutions of the PDE.

3. Model calculations

Response to $I(t)$. We apply the pulse input signal given by

$$I(t) = \Delta I\Theta(t-2)\Theta(6-t), \quad (94)$$

where $\Delta I=1.0$ and $\Theta(t)$ denotes the Heaviside function: $\Theta(t)=1$ for $t>0$ and zero otherwise. Figure 7 shows the time-dependent distribution at various t for $\lambda=1.0$, $\alpha=0.5$, $\beta=0.5$, and $J=0.0$. Solid and dashed curves express the results of the PDE method and the analytical method (Sec. II F 1), respectively. When input of ΔI is applied at $t=2.0$, the distribution is gradually changed, moving rightward. The results of the analytical method are in good agreement with those obtained by the PDE method, except for $t=3$ and $t=7$.

This change in $p(x,t)$ induces changes in $\mu_q(t)$, $\sigma_q(t)^2$, $S_q(t)$, and $g_q(t)$, whose time dependences are shown in Figs. 8(a) and 8(b), solid and dashed curves expressing the results of the PDE method and the analytical method, respectively. By an applied pulse input, μ_q, σ_q^2, and S_q are increased while g_q is decreased. The result for $S_q(t)$ of the analytical method is in fairly good agreement with that obtained by the PDE method. The calculated $g_q(t)$ of the analytical method is also in good agreement with that of the PDE method besides near the transient periods at $t \gtrsim 2$ and $t \gtrsim 6$ just after the input signal is on and off. This is expected due to the fact that $g_q(t)$ given by Eq. (71) is sensitive to a detailed form of $p(x,t)$ because it is expressed by an integration of $[\partial p(x,t)/\partial x]^2$ over $p(x,t)$, while $S_q(t)$ is obtained by a simple integration of $p(x,t)^q$.

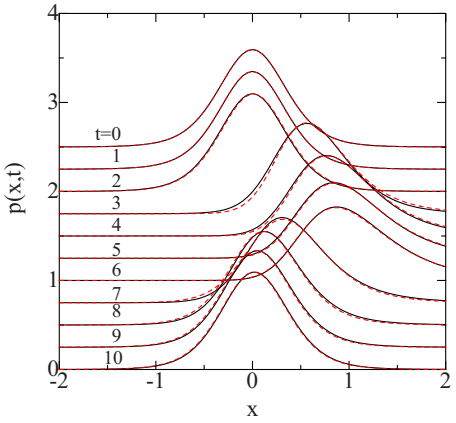

FIG. 7. (Color online) The time-dependent probability distribution $p(x,t)$ when an input pulse given by $I(t)=\Delta I\Theta(t-2)\Theta(6-t)$ is applied with $\Delta I=1.0$, $\lambda=1.0$, $\alpha=0.5$, and $\beta=0.5$: Solid curves express the results obtained by the PDE method and chain curves denote those by the analytical method described in Sec. II F 1. Curves are consecutively shifted downward by 0.25 for clarity of the figure.

For a comparison, we show by chain curves the results of the PDE method when the step input given by

$$I(t) = \Delta I\Theta(t-2) \quad (95)$$

is applied. The relaxation time of S_q and g_q is about 2.0.

It is noted that input signal for $\alpha=0$ induces no changes in $S_q(t)$ and $g_q(t)$, which has been already realized in the stationary state as shown by chain curves in Figs. 4(c) and 4(d).

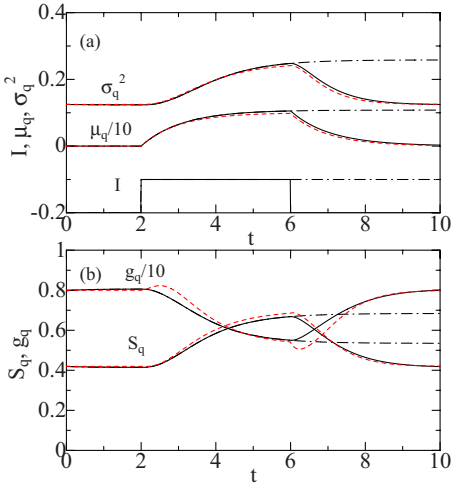

FIG. 8. (Color online) The time dependence of (a) $\mu_q(t)$ and $\sigma_q(t)^2$ and (b) $S_q(t)$ and $g_q(t)$ for an input of $I(t)=\Delta I\Theta(t-2)\Theta(6-t)$ with $\Delta I=1.0$, $\lambda=1.0$, $\alpha=0.5$, $\beta=0.5$, and $J=0.0$. Solid curves denote the results obtained by the PDE method and dashed curves those obtained by the analytical method described in Sec. II F 1. Chain curves denote the results of the PDE method for an input signal given by $I(t)=\Delta I\Theta(t-2)$, results of g_q and μ_q being divided by a factor of 10.

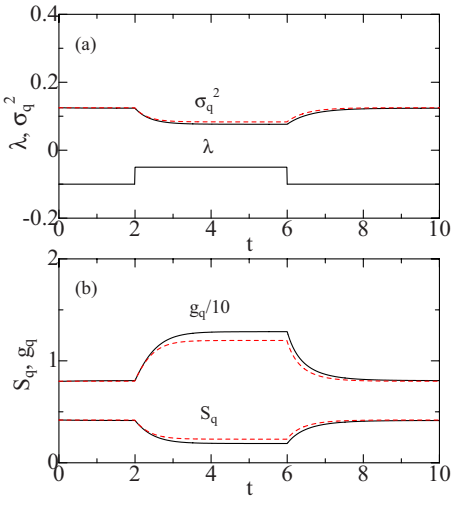

FIG. 9. (Color online) The time dependence of (a) $\sigma_q(t)^2$ and (b) $S_q(t)$ and $g_q(t)$ for $\lambda(t)=1.0+\Delta\lambda\Theta(t-2)\Theta(6-t)$: $\Delta\lambda=0.5$, $\alpha=0.5$, $\beta=0.5$, $I=0.0$, and $J=0.0$. Solid curves denote the results obtained by the PDE method and dashed curves those obtained by the analytical method described in Sec. II F 1, results of g_q being divided by a factor of 10.

Response to $\lambda(t)$. We modify the relaxation rate as given by

$$\lambda = 1.0 + \Delta\lambda\Theta(t-2)\Theta(6-t), \tag{96}$$

which expresses an application of an external force of ΔF $(=-\Delta\lambda x)$ at $2\leq t<6$ with $\Delta\lambda=0.5$. Figures 9(a) and 9(b) show the time dependence of σ_q^2, S_q, and g_q with $\alpha=0.5$, $\beta=0.5$, $I=0.0$, and $J=0.0$ for which $\mu_q=0$. Solid and dashed curves express the results of the PDE method and the analytical method, respectively. When an external force is applied, σ_q^2 and S_q are decreased whereas g_q is increased. The results of the analytical method are in good agreement with those of the PDE method. The relaxation times of S_q and g_q are 0.47 and 0.53, respectively.

III. DISCUSSION

A. Maximum-entropy method

In Sec. II we have discussed the information entropies by using the probability distribution obtained by the FPE for the Langevin model. It is worthwhile to compare it with the probability distribution derived by the MEM. The variational condition for the Tsallis entropy given by Eq. (1) is taken into account with the three constraints: A normalization condition and q moments of x and x^2, as given by [14,17,18,36]

$$1 = \int p(x)dx, \tag{97}$$

$$\mu_q = E_q[x] = \int P_q(x)xdx, \tag{98}$$

$$\sigma_q^2 = E_q[(x-\mu_q)^2] = \int P_q(x)(x-\mu_q)^2dx, \tag{99}$$

where $E_q[\cdots]$ expresses the average over the escort probability of $P_q(x)$ given by

$$P_q(x) = \frac{p(x)^q}{c_q}, \tag{100}$$

$$c_q = \int p(x)^q dx, \tag{101}$$

the entropic index q being assumed to be $0<q<3$. After some manipulations, we get the q-Gaussian (non-Gaussian) distribution given by [36]

$$p(x) = \frac{1}{Z_q}\exp_q\left(-\frac{(x-\mu_q)^2}{2\nu\sigma_q^2}\right), \tag{102}$$

with

$$\nu = \left(\frac{3-q}{2}\right), \tag{103}$$

$$Z_q = \int \exp_q\left(-\frac{(x-\mu_q)^2}{2\nu\sigma_q^2}\right)dx \tag{104}$$

$$= \left(\frac{2\nu\sigma_q^2}{q-1}\right)^{1/2} B\left(\frac{1}{2}, \frac{1}{q-1}-\frac{1}{2}\right) \quad \text{for } 1<q<3, \tag{105}$$

$$= \sqrt{2\pi}\sigma_1 \quad \text{for } q=1, \tag{106}$$

$$= \left(\frac{2\nu\sigma_q^2}{1-q}\right)^{1/2} B\left(\frac{1}{2}, \frac{1}{1-q}+1\right) \quad \text{for } 0<q<1. \tag{107}$$

In the limit of $q\to 1$, $p(x)$ in Eq. (102) becomes the Gaussian distribution,

$$p(x) = \frac{1}{\sqrt{2\pi}\sigma_1}e^{-(x-\mu_1)^2/2\sigma_1^2}. \tag{108}$$

The probability distribution given by Eq. (102) derived from the MEM is different from that of Eq. (34) obtained by the FPE although both expressions are equivalent for $\mu_q=I=J=0$ with $\nu\sigma_q^2=\phi^2$. Note that the former is defined for $0<q<3$ while the latter is valid for $1\leq q<3$.

A comparison between the probability distributions obtained by the FPE and MEM is made in Figs. 10 and 11. Figure 10(a) shows the probability distributions calculated by the FPE of the Langevin model for $\alpha=0.0$, 0.5, 1.0, 1.5, and 2.0, which yield $(q,\sigma_q^2)=(1.0,0.125)$, (1.222,0.25), (1.667,0.625), (2.059,1.25), and (2.333,2.125), respectively, with $\mu_q=1.0$ for $I=1.0$, $\lambda=1.0$, $\beta=0.5$, and $J=0.0$ [Eqs. (84) and (85)]. Figure 10(b) shows corresponding distributions calculated by the MEM with the respective parameters of μ_q, σ_q, and q. For $q=1.0$ $(\alpha=0.0)$, both the distributions are Gaussian centered at $x=\mu_q=1.0$. For $q\neq 1.0$, $p(x)$ of the FPE becomes asymmetric with respect to its peak while that of the MEM is still symmetric. The peak position of $p(x)$ of the

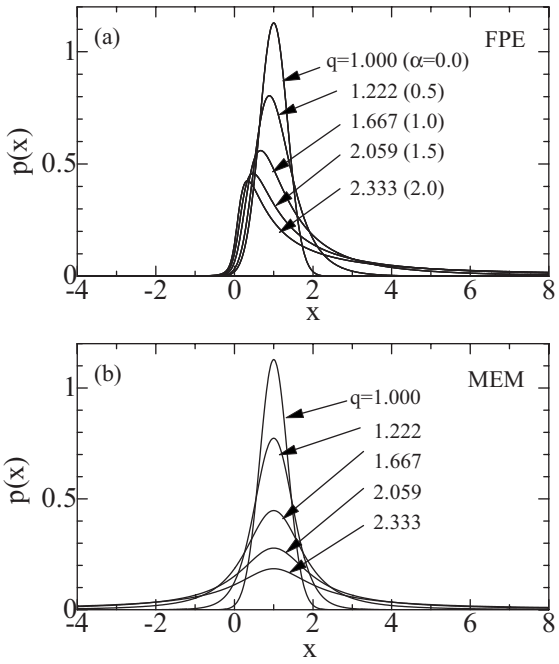

FIG. 10. Probability distributions $p(x)$ calculated by (a) the FPE and (b) MEM for $(\alpha, q, \sigma_q^2)=(0.0, 1.000, 0.125)$, (0.5,1.222,0.25), (1.0,1.667,0.625), (1.5,2.059,1.25), and (2.0,2.333,2.125) with $I=1.0$, $\lambda=1.0$, $\beta=0.5$, and $J=0.0$: The figures in parentheses of (a) denote α values.

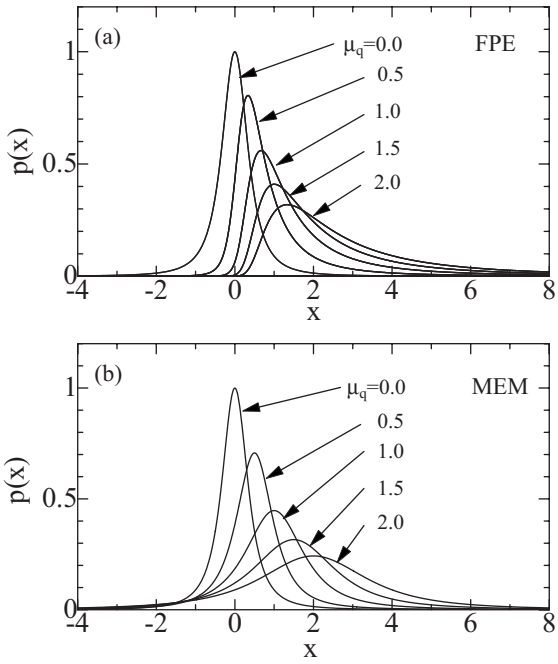

FIG. 11. Probability distributions $p(x)$ calculated by (a) the FPE and (b) MEM for $(\mu_q, \sigma_q^2)=(0.0, 0.125)$, (0.5,0.25), (1.0,0.625), (1.5,1.25), and (2.0,2.125), respectively, with $\lambda=1.0$, $\alpha=1.0$, $\beta=0.5$, and $J=0.0$.

MEM is at $x=\mu_q=1.0$ independent of q while that of the FPE moves leftward with increasing α. It is noted that $p(x)$ of the FPE for $\alpha\neq 0$ and $\beta=0$ given by Eq. (39) has a peak at $x=\mu_q/q$.

Figure 11(a) shows $p(x)$ of the FPE for various inputs of $I=0.0$, 0.5, 1.0, 1.5, and 2.0, which yield $(\mu_q, \sigma_q^2)=(0.0, 0.125)$, (0.5,0.25), (1.0,0.625), (1.5,1.25), and (2.0,2.125), respectively, for $\lambda=1.0$, $\alpha=1.0$, $\beta=0.5$, and $J=0.0$ [Eqs. (84) and (85)]: Corresponding $p(x)$ of the MEM with the respective parameters of μ_q, σ_q, and $q(=1.667)$ are plotted in Fig. 11(b). For $\mu_q=0.0$, both the distributions agree. Although centers of both distributions move rightward with increasing μ_q, their profiles and peak positions are different between the two distributions. We note that the magnitude of $p(x)$ at $x<0.0$ of the FPE is smaller than that of the MEM for $\mu_q\neq 0.0$.

The information entropies calculated with the use of the distribution given by Eq. (102) are summarized in the Appendix. One of the advantages of the MEM is that its distribution is explicitly specified by the parameters of $(\theta_1, \theta_2)=(\mu_q, \sigma_q^2)$ while that of the FPE is given in an implicit way [cf. Eqs. (86)–(88)]. We may discuss the upper bound of estimation errors by the Cramér-Rao inequality, which is shown to be expressed by the extended Fisher entropy [Eq. (A19)] but not by the generalized Fisher entropy [Eq. (A6)].

In order to discuss the dynamics within the MEM for $q\neq 1.0$, we have once tried to obtain an analytic solution of its distribution $p(x,t)$, assuming that it is given by Eq. (102),

$$p(x,t)=\left(\frac{A_q}{\sqrt{\sigma_q(t)^2}}\right)\exp_q\left(-\frac{[x-\mu_q(t)]^2}{2\nu\sigma_q(t)^2}\right), \tag{109}$$

where the q-dependent coefficient A_q is determined from Eqs. (105)–(107), and equations of motion for $\mu_q(t)$ and $\sigma_q(t)^2$ are derived so as to meet the FPE after Refs. [17,18]. Unfortunately, we could not uniquely determine them: We obtained two equations for $d\mu_q(t)/dt$ and three equations for $d\sigma_q(t)^2/dt$ which are mutually not consistent (except for $q=1.0$). This implies that the exact analytic solution of the FPE is not given by Eq. (109). Indeed, the exact solution for $\beta=J=0$ in Eq. (26) does not have a functional form given by Eq. (109) [37].

B. Entropy flux and entropy production

It is interesting to discuss the entropy flux and entropy production from the time derivative of the Tsallis entropy given by

$$\frac{dS_q(t)}{dt}=-\left(\frac{q}{q-1}\right)\int p(x,t)^{q-1}\left(\frac{\partial p(x,t)}{\partial t}\right)dx \tag{110}$$

$$=Q_F+Q_A+Q_M, \tag{111}$$

with

$$Q_F=q\int p(x,t)^q\left(\frac{dF(x)}{dx}\right)dx + q(q-1)\int p(x,t)^q\left(\frac{\partial \ln p(x,t)}{\partial x}\right)F(x)dx, \tag{112}$$

$$Q_A = \left(\frac{\alpha^2 q}{2}\right)\int p(x,t)^q \left(\frac{\partial \ln p(x,t)}{\partial x}\right)^2 dx, \tag{113}$$

$$Q_M = \left(\frac{\beta^2}{2}\right)\int p(x,t)^q \left[q\left(\frac{\partial \ln p(x,t)}{\partial x}\right)^2 G(x)^2 - \left(\frac{dG(x)}{dx}\right)^2 - \frac{d^2G(x)}{dx^2}G(x)\right]dx. \tag{114}$$

Here Q_F denotes the entropy flux, and Q_A and Q_M stand for entropy productions due to additive and multiplicative noise, respectively.

By using the stationary distribution given by Eq. (46), we obtain Q_F, Q_A, and Q_M in the stationary state with $I=J=0$ (i.e., without couplings and external input),

$$Q_F = -\frac{\lambda q}{Z_q^q}\left(\frac{2\sigma_q^2}{q-1}\right)^{1/2} B\left(\frac{1}{2}, \frac{1}{q-1}+\frac{1}{2}\right) + \frac{\lambda q(q-1)}{\sigma_q^2 Z_q^q}\left(\frac{2\sigma_q^2}{q-1}\right)^{3/2} B\left(\frac{3}{2}, \frac{1}{q-1}+\frac{1}{2}\right), \tag{115}$$

$$Q_A = \frac{\beta^2 q}{2\sigma_q^4 Z_q^q}\left(\frac{2\sigma_q^2}{q-1}\right)^{3/2} B\left(\frac{3}{2}, \frac{1}{q-1}+\frac{3}{2}\right), \tag{116}$$

$$Q_M = \frac{\alpha^2 q}{2\sigma_q^4 Z_q^q}\left(\frac{2\sigma_q^2}{q-1}\right)^{5/2} B\left(\frac{5}{2}, \frac{1}{q-1}+\frac{1}{2}\right) - \frac{\alpha^2}{2Z_q^q}\left(\frac{2\sigma_q^2}{q-1}\right)^{1/2} B\left(\frac{1}{2}, \frac{1}{q-1}+\frac{1}{2}\right), \tag{117}$$

where Z_q is given by Eq. (47). Equations (115)–(117) satisfy the stationary condition, $Q_F+Q_A+Q_M=0$.

It is worthwhile to examine the limit of $\alpha \to 0$ ($q \to 1.0$), in which Eqs. (110) and (115)–(117) yield

$$\frac{dS_1(t)}{dt} = -\int \frac{\partial p(x,t)}{\partial t} \ln p(x,t) dx \tag{118}$$

$$= Q_F + Q_A, \tag{119}$$

with

$$Q_F = \int p(x,t)\left(\frac{dF(x)}{dx}\right)dx, \tag{120}$$

$$Q_A = \left(\frac{\alpha^2}{2}\right)\int p(x,t)\left(\frac{\partial \ln p(x,t)}{\partial x}\right)^2 dx. \tag{121}$$

With noticing the relation $\lim_{|z|\to\infty}[\Gamma(z+a)/\Gamma(z)z^a]=1$ [38], we may see that Eqs. (120) and (121) lead to $Q_F=-Q_A=-\lambda$ and $dS_1/dt=0$ in the limit of $q \to 1$.

In the opposite limit of $\beta \to 0$, Eqs. (115)–(117) yield that each of Q_F, Q_A, and Q_M is proportional to $1/\beta^{(q-1)}$ and then divergent in this limit, though $Q_F+Q_A+Q_M=0$. It is noted that $Q_A=\lambda$ for $\alpha \to 0$ and $\beta \to 0$ [2–4].

We present some model calculations of Q_F, Q_A, and Q_M in the stationary state, which are shown in Fig. 12 as a function of α for $\beta=0.1$ (dashed curves), $\beta=0.5$ (chain curves), and $\beta=1.0$ (solid curves). We note that $Q_F<0$ and $Q_A+Q_M>0$. With increasing α, Q_F is decreased in the case of $\beta=0.1$, while it is increased in the cases of $\beta=0.5$ and 1.0. Bag [4] showed that Q_F is always decreased with increasing α which disagrees with our result mentioned above: Equations (115)–(117) are rather different from Eqs. (36) and (37) in Ref. [4] where non-Gaussian properties of the distribution are not properly taken into account.

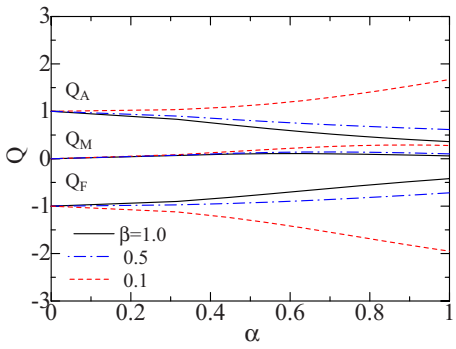

FIG. 12. (Color online) The α dependence of entropy flux (Q_F), and entropy productions by additive noise (Q_A) and multiplicative noise (Q_M) for $\beta=0.1$ (dashed curves), $\beta=0.5$ (chain curves), and $\beta=1.0$ (solid curves) with $\lambda=1.0$, $I=0.0$, and $J=0.0$.

C. q-moment and normal-moment methods

In Refs. [30,32], we have discussed equations of motion for normal moments of μ ($=E[x]$) and σ^2 ($=E[(x-\mu)^2]$) [Eq. (50)] in the Langevin model with $J=0$, as given by

$$\frac{d\mu(t)}{dt} = -\left(\lambda - \frac{\alpha^2}{2}\right)\mu(t) + I, \tag{122}$$

$$\frac{d\sigma(t)^2}{dt} = -2(\lambda-\alpha^2)\sigma(t)^2 + \alpha^2\mu(t)^2 + \beta^2. \tag{123}$$

These equations of motion are rather different from those for the q moments of μ_q and σ_q^2 given by Eqs. (82) and (83). Indeed, Eqs. (122) and (123) yield stationary normal moments given by

$$\mu = \frac{I}{(\lambda - \alpha^2/2)}, \tag{124}$$

$$\sigma^2 = \frac{(\alpha^2\mu^2 + \beta^2)}{2(\lambda-\alpha^2)}, \tag{125}$$

which are different from the stationary q moments of μ_q and σ_q^2 given by Eqs. (84) and (85), and which diverge at $\lambda=\alpha^2/2$ and $\lambda=\alpha^2$, respectively.

The time dependence of $\mu(t)$ and $\sigma(t)^2$ becomes considerably different from those of $\mu_q(t)$ and $\sigma_q(t)^2$ for an appreciable value of α. Figures 13(a)–13(d) show some examples of $\mu_q(t)$, $\sigma_q(t)^2$, $\mu(t)$, and $\sigma(t)^2$, respectively, when a pulse input given by Eq. (94) is applied with $\alpha=0.2$ (chain curves), $\alpha=0.5$ (dashed curves), and $\alpha=0.8$ (solid curves). Although $\mu_q(t)$ is independent of α, $\sigma_q(t)^2$, $\mu(t)$, and $\sigma(t)^2$ are much

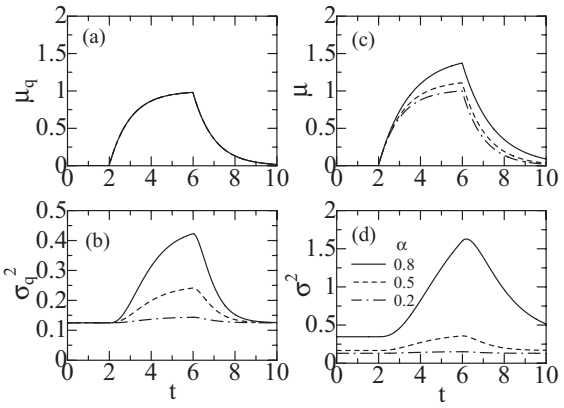

FIG. 13. The time dependence of q moments of (a) $\mu_q(t)$ and (b) $\sigma_q(t)^2$, and those of normal moments of (c) $\mu(t)$ and (d) $\sigma(t)^2$ with $\alpha=0.2$ (chain curves), $\alpha=0.5$ (dashed curves), and $\alpha=0.8$ (solid curves) for an input given by $I(t)=\Delta I\Theta(t-2)\Theta(6-t)$ with $\Delta I=1.0$, $\lambda=1.0$, $\beta=0.5$, and $J=0.0$. The vertical scale of (b) is different from those of (a), (c), and (d).

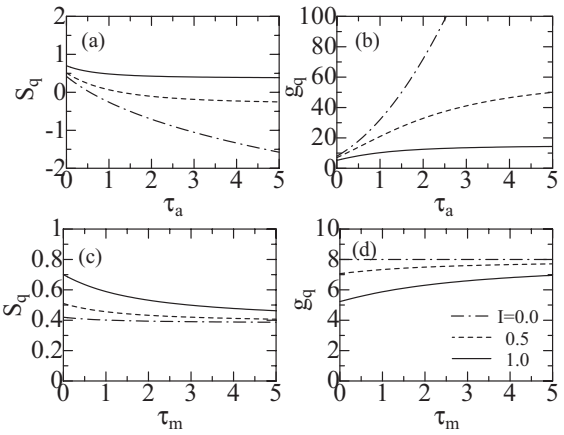

FIG. 14. The τ_a dependence of (a) S_q and (b) g_q with $\tau_m=0.0$ and the τ_m dependence of (c) S_q and (d) g_q with $\tau_a=0.0$: $I=0.0$ (chain curves), $I=0.5$ (dashed curves), and $I=1.0$ (solid curves) with $\lambda=1.0$, $\alpha=0.5$, and $\beta=0.5$.

increased at $2\leq t<6$ for larger α. In particular, $\sigma(t)^2$ is significantly increased because of the α^2 term in Eq. (123).

D. Effects of colored noise

We have so far considered additive and multiplicative white noise. In our recent paper [33], we have taken into account the effect of colored noise by employing the functional-integral method. We have assumed the Langevin model subjected to additive (χ) and multiplicative (ϕ) colored noise given by

$$\frac{dx(t)}{dt}=-\lambda x(t)+\chi(t)+x(t)\phi(t)+I(t), \tag{126}$$

with

$$\frac{d\chi(t)}{dt}=-\frac{1}{\tau_a}[\chi(t)-\beta\xi(t)], \tag{127}$$

$$\frac{d\phi(t)}{dt}=-\frac{1}{\tau_m}[\phi(t)-\alpha\eta(t)], \tag{128}$$

where τ_a and β (τ_m and α) express the relaxation time and strength of additive (multiplicative) noise, respectively, and ξ and η stand for independent zero-mean Gaussian white noise. Formally the probability distribution of $p(x,\chi,\phi,t)$ for the Langevin model given by Eqs. (126)–(128) is expressed by the multivariate FPE. Applying the functional-integral method to the Langevin model, we have obtained the effective one-variable FPE, from which the effective Langevin model is derived as [33]

$$\frac{dx(t)}{dt}=-\lambda x(t)+\tilde{\beta}\xi(t)+\tilde{\alpha}(t)x(t)\eta(t)+I(t), \tag{129}$$

with

$$\tilde{\beta}^2=\frac{\beta^2}{(1+\lambda\tau_a)}, \tag{130}$$

$$\tilde{\alpha}(t)^2=\frac{\alpha^2}{[1+\tau_m I(t)/\mu(t)]}. \tag{131}$$

Here $\mu(t)$ is given by Eq. (122) with $\alpha=\tilde{\alpha}$, from which $\tilde{\alpha}$ is determined in a self-consistent way.

In the stationary state where $\mu=I/(\lambda-\tilde{\alpha}^2/2)$ given by Eq. (124) with $\alpha=\tilde{\alpha}$, we obtain $\tilde{\alpha}$ from Eq. (131),

$$\tilde{\alpha}^2=\frac{\alpha^2}{[1+\tau_m(\lambda-\tilde{\alpha}^2/2)]} \tag{132}$$

$$=\frac{1}{\tau_m}[(1+\lambda\tau_m)-\sqrt{(1+\lambda\tau_m)^2-2\tau_m\alpha^2}]. \tag{133}$$

We get an approximate expression given by [33]

$$\tilde{\alpha}^2\simeq\frac{\alpha^2}{(1+\lambda\tau_m)} \quad \text{for} \quad \tau_m\alpha^2/2(1+\lambda\tau_m)^2\ll 1, \tag{134}$$

which is shown to be a good approximation both for $\tau_m\ll(1/\lambda,2/\alpha^2)$ and $\tau_m\gg(1/\lambda,\alpha^2/2\lambda^2)$ [33]. Equations (130) and (134) show that effects of additive and multiplicative colored noise are described by $\tilde{\alpha}^2$ and $\tilde{\beta}^2$ which are reduced by factors of $(1+\lambda\tau_a)$ and $(1+\lambda\tau_m)$, respectively, from original values of α^2 and β^2.

The τ_a dependence of S_q and g_q is plotted in Figs. 14(c) and 14(d) with $\tau_m=0.0$ for $I=0.0$ (chain curves), $I=0.5$ (dashed curves), and $I=1.0$ (solid curves) with $\lambda=1.0$, $\alpha=0.5$, and $\beta=0.5$. We note that with increasing τ_a, g_q is much increased for smaller I whereas S_q is much decreased for smaller I. The dependence of S_q and g_q on τ_a may be understood from their β dependence shown in Figs. 3(c) and 3(d). The τ_m dependence of S_q and g_q is plotted in Figs. 14(c) and 14(d) with $\tau_a=0.0$ with $\lambda=1.0$, $\alpha=0.5$, and $\beta=0.5$. With increasing τ_m, $S_q(g_q)$ is decreased (increased) for $I=0.5$ and $I=1.0$ while no changes for $I=0.0$. This behavior may be explained from Figs. 2(c) and 2(d) showing the α dependence of S_q and g_q.

IV. CONCLUSION

We have discussed stationary and dynamical properties of the Tsallis and Fisher entropies in nonextensive systems. Our calculation for the N-unit coupled Langevin model subjected to additive and multiplicative noise has shown the following:

(i) The dependence of S_q and g_q on the parameters of λ, α, β, I, J, and N in the coupled Langevin model are clarified (Figs. 2–6).

(ii) Dynamical properties are well described by the analytical method for the FPE proposed in Sec. II F 1, which shows that the relaxation times in transient responses of S_q and g_q to a change in λ are short ($\tau \sim 0.5$) while those in I are fairly long ($\tau \sim 2$).

The difference between the parameter dependence of S_q and g_q in the item (i) arises from the fact that S_q provides us with a global measure of ignorance while g_q a local measure of positive amount of information [1].

We have calculated the information entropies also by using the probability distribution derived by the MEM, from which we obtain the following:

(iii) $p(x)$ derived by the MEM is rather different from that of the FPE for $\mu_q \neq 0$ (Figs. 10 and 11), for which the information entropies of the MEM are independent of μ_q while those of the FPE depend on μ_q (i.e., I).

(iv) The Cramér-Rao inequality is expressed by the extended Fisher entropy [Eq. (A19)] which is different from the generalized Fisher entropy [Eq. (A6)] derived from the generalized Kullback-Leibler divergence [Eq. (6)].

The item (iv) has not been clarified in previous studies on the Fisher entropies in nonextensive systems [13–24].

The Langevin model has been employed for a study of a wide range of stochastic systems [29]. Quite recently, the present author has proposed the generalized rate-code model for neuronal ensembles which is described by the coupled Langevin-type equation [39,40]. It would be interesting to discuss the dynamics of information entropies in such neural networks, which is left for our future study.

ACKNOWLEDGMENTS

This work is partly supported by a Grant-in-Aid for Scientific Research from the Japanese Ministry of Education, Culture, Sports, Science and Technology.

APPENDIX: MAXIMUM-ENTROPY METHOD

By using the probability distribution given by Eq. (102) derived by the MEM, we have calculated the information entropies, which are summarized in this appendix.

1. Tsallis entropy

With the use of Eqs. (1) and (102), the Tsallis entropy is given by

$$S_q = \left(\frac{1}{2}\right)[1 + \ln(2\pi\sigma_q^2)] \quad \text{for } q = 1, \tag{A1}$$

$$= \left(\frac{1 - c_q}{q - 1}\right) \quad \text{for } q \neq 1, \tag{A2}$$

with

$$c_q = \frac{1}{Z_q^q}\left(\frac{2\nu\sigma_q^2}{q-1}\right)^{1/2} B\left(\frac{1}{2}, \frac{q}{q-1} - \frac{1}{2}\right) \quad \text{for } 1 < q < 3, \tag{A3}$$

$$= \frac{1}{Z_q^q}\left(\frac{2\nu\sigma_q^2}{1-q}\right)^{1/2} B\left(\frac{1}{2}, \frac{q}{1-q} + 1\right) \quad \text{for } 0 < q < 1, \tag{A4}$$

which yield

$$c_q = \nu Z_q^{1-q} \quad \text{for } 0 < q < 3. \tag{A5}$$

Here Z_q for $0 < q < 1$ and $1 < q < 3$ are given by Eqs. (105) and (107), respectively.

2. Generalized Fisher entropy

The distribution $p(x)$ given by Eq. (102) is characterized by two parameters of $(\theta_1, \theta_2) = (\mu_q, \sigma_q^2)$. By using Eqs. (4) and (102), we obtain the component of the generalized Fisher information matrix $\mathbf{G}$ given by [16–24]

$$g_{ij} = qE\left[\left(\frac{\partial \ln p(x)}{\partial \theta_i}\right)\left(\frac{\partial \ln p(x)}{\partial \theta_j}\right)\right] \tag{A6}$$

$$= qE[(X_i - E[X_i])(X_j - E[X_j])] \quad \text{for } i,j = 1,2, \tag{A7}$$

with

$$X_i = \frac{\partial}{\partial \theta_i} \ln\left[\exp_q\left(-\frac{(x-\mu_q)^2}{2\nu\sigma_q^2}\right)\right], \tag{A8}$$

where $E[\cdots]$ denotes the average over the q-Gaussian distribution of $p(x)$ whereas $E_q[\cdots]$ stands for the average over the escort distribution of $P_q(x)$. Substituting the probability given by Eq. (102) to Eq. (A6), we obtain

$$g_{11} = q\int p(x)\left(\frac{\partial \ln p(x)}{\partial \mu_q}\right)^2 dx \tag{A9}$$

$$= q\int p(x)\left(\frac{\partial \ln p(x)}{\partial x}\right)^2 dx \tag{A10}$$

$$= \left(\frac{2q}{\nu\sigma_q^2(q-1)}\right)\frac{B\left(\frac{3}{2}, \frac{1}{(q-1)} + \frac{1}{2}\right)}{B\left(\frac{1}{2}, \frac{1}{(q-1)} - \frac{1}{2}\right)} \quad \text{for } 1 < q < 3, \tag{A11}$$

$$= \frac{1}{\sigma_q^2} \quad \text{for } q = 1, \tag{A12}$$

$$= \left(\frac{2q}{\nu \sigma_q^2 (1-q)} \right) \frac{B\left(\frac{3}{2}, \frac{1}{(1-q)} - 1 \right)}{B\left(\frac{1}{2}, \frac{1}{(1-q)} + 1 \right)} \quad \text{for } 0 < q < 1, \tag{A13}$$

which yield

$$g_{11} = \frac{1}{\sigma_q^2} \quad \text{for } 0 < q < 3. \tag{A14}$$

A similar calculation leads to the (2,2) component given by

$$g_{22} = q \int p(x) \left(\frac{\partial \ln p(x)}{\partial \sigma_q^2} \right)^2 dx \tag{A15}$$

$$= \left(\frac{3-q}{4\sigma_q^4} \right) \quad \text{for } 0 < q < 3. \tag{A16}$$

The generalized Fisher information matrix is expressed by

$$\mathbf{G} = \begin{pmatrix} \frac{1}{\sigma_q^2} & 0 \\ 0 & \frac{(3-q)}{4\sigma_q^4} \end{pmatrix},$$

whose inverse is given by

$$\mathbf{G}^{-1} = \begin{pmatrix} \sigma_q^2 & 0 \\ 0 & \frac{4\sigma_q^4}{(3-q)} \end{pmatrix}.$$

In the limit of $q=1$, the matrix reduces to

$$\mathbf{G} = \begin{pmatrix} \frac{1}{\sigma_1^2} & 0 \\ 0 & \frac{1}{2\sigma_1^4} \end{pmatrix} \quad \text{for } q = 1.$$

3. Extended Fisher entropy: Cramér-Rao inequality

Next we discuss the Cramér-Rao inequality in nonextensive systems. For the escort distribution given by Eq. (100) which satisfies Eqs. (98) and (99) with

$$1 = E_q[1] = \int P_q(x) dx, \tag{A17}$$

we get the Cramér-Rao inequality [1,16,20,21]

$$\mathbf{V} \geq \tilde{\mathbf{G}}^{-1}. \tag{A18}$$

Here $\mathbf{V}$ denotes the covariance error matrix whose explicit expression will be given shortly, and $\tilde{\mathbf{G}}$ is referred to as the extended Fisher information matrix whose components are expressed by

$$\tilde{g}_{ij} = E_q \left[\left(\frac{\partial \ln P_q(x)}{\partial \theta_i} \right) \left(\frac{\partial \ln P_q(x)}{\partial \theta_j} \right) \right] \quad \text{for } i,j = 1,2, \tag{A19}$$

$$= E_q[(\tilde{X}_i - E_q[\tilde{X}_i])(\tilde{X}_j - E_q[\tilde{X}_j])], \tag{A20}$$

with

$$\tilde{X}_i = \frac{\partial}{\partial \theta_i} [q \ln p(x)] \tag{A21}$$

$$= q(X_i - E[X_i]), \tag{A22}$$

X_i being given by Eq. (A8). Note that $\tilde{g}_{ij}$ is different from g_{ij} given by Eq. (A6) except for $q=1.0$. The (1,1) component of $\tilde{\mathbf{G}}$ is given by

$$\tilde{g}_{11} = E_q \left[\left(\frac{\partial \ln P_q(x)}{\partial \mu_q} \right)^2 \right] \tag{A23}$$

$$= \left(\frac{q^2}{c_q} \right) \int p(x)^q \left(\frac{\partial \ln p(x)}{\partial x} \right)^2 dx \tag{A24}$$

$$= \left(\frac{2q^2}{\nu \sigma_q^2 (q-1)} \right) \frac{B\left(\frac{3}{2}, \frac{q}{(q-1)} + \frac{1}{2} \right)}{B\left(\frac{1}{2}, \frac{q}{(q-1)} - \frac{1}{2} \right)} \quad \text{for } 1 < q < 3, \tag{A25}$$

$$= \frac{1}{\sigma_q^2} \quad \text{for } q = 1, \tag{A26}$$

$$= \left(\frac{2q^2}{\nu \sigma_q^2 (1-q)} \right) \frac{B\left(\frac{3}{2}, \frac{q}{(1-q)} - 1 \right)}{B\left(\frac{1}{2}, \frac{q}{(1-q)} + 1 \right)} \quad \text{for } 1/2 < q < 1, \tag{A27}$$

which lead to

$$\tilde{g}_{11} = \frac{q(q+1)}{(3-q)(2q-1)\sigma_q^2} \quad \text{for } 1/2 < q < 3. \tag{A28}$$

Similarly, the (2,2) component of $\tilde{\mathbf{G}}$ is given by

$$\tilde{g}_{22} = E_q \left[\left(\frac{\partial \ln P_q(x)}{\partial \sigma_q^2} \right)^2 \right] \tag{A29}$$

$$= \frac{(q+1)}{4(2q-1)\sigma_q^4} \quad \text{for } 1/2 < q < 3. \tag{A30}$$

The extended Fisher information matrix $\tilde{\mathbf{G}}$ is expressed by

$$\tilde{\mathbf{G}} = \begin{pmatrix} \frac{q(q+1)}{(3-q)(2q-1)\sigma_q^2} & 0 \\ 0 & \frac{(q+1)}{4(2q-1)\sigma_q^4} \end{pmatrix},$$

whose inverse is given by

$$\tilde{\mathbf{G}}^{-1} = \begin{pmatrix} \dfrac{(3-q)(2q-1)\sigma_q^2}{q(q+1)} & 0 \\ 0 & \dfrac{4(2q-1)\sigma_q^4}{(q+1)} \end{pmatrix}.$$

A calculation of the (i,j) component (v_{ij}) of the covariance error matrix $\mathbf{V}$ leads to

$$\mathbf{V} = \begin{pmatrix} \sigma_q^2 & 0 \\ 0 & \dfrac{4\sigma_q^4}{(5-3q)} \end{pmatrix}.$$

In the limit of $q=1$, the matrices reduce to

$$\tilde{\mathbf{G}}^{-1} = \mathbf{G}^{-1} = \begin{pmatrix} \sigma_1^2 & 0 \\ 0 & 2\sigma_1^4 \end{pmatrix} \quad \text{for } q=1,$$

$$\mathbf{V} = \begin{pmatrix} \sigma_1^2 & 0 \\ 0 & 2\sigma_1^4 \end{pmatrix} \quad \text{for } q=1.$$

Chain and solid curves in Fig. 15(a) express the q dependence of v_{11}/σ_q^2 and $1/\tilde{g}_{11}\sigma_q^2$, respectively. When q is further from unity, $1/\tilde{g}_{11}$ is much decreased and it vanishes at $q=1/2$ and 3. The lower bond of v_{11} is expressed by the Cramér-Rao relation because it is satisfied by $\tilde{g}_{11}$,

$$v_{11} = \frac{1}{g_{11}} \geq \frac{1}{\tilde{g}_{11}} \quad \text{for } 1/2 < q < 3. \tag{A31}$$

Chain, dashed, and solid curves in Fig. 15(b) show v_{22}/σ_q^4, $1/g_{22}\sigma_q^4$, and $1/\tilde{g}_{22}\sigma_q^4$, respectively. It is noted that v_{22} diverges at $q=5/3$. The following relations hold:

$$\frac{1}{g_{22}} > v_{22} > \frac{1}{\tilde{g}_{22}} \quad \text{for } 1/2 < q < 1, \tag{A32}$$

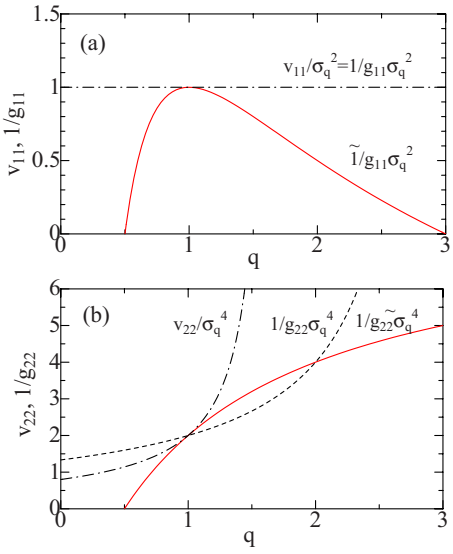

FIG. 15. (Color online) The q dependence of (a) v_{11}/σ_q^2 $(=1/g_{11}\sigma_q^2)$ (chain curve) and $1/\tilde{g}_{11}\sigma_q^2$ (solid curve), and (b) v_{22}/σ_q^4 (chain curve), $1/\tilde{g}_{22}\sigma_q^4$ (solid curve), and $1/g_{22}\sigma_q^4$ (dashed curve): g_{ij} and $\tilde{g}_{ij}$ are elements of the generalized and extended Fisher information matrices, respectively.

$$v_{22} \geq \frac{1}{\tilde{g}_{22}} \geq \frac{1}{g_{22}} \quad \text{for } 1 \leq q < 5/3. \tag{A33}$$

Equation (A32) means that $1/g_{22}$ cannot provide the lower bound of v_{22}. Equations (A31)–(A33) clearly show that the lower bound of $\mathbf{V}$ is expressed by the extended Fisher information matrix $\tilde{\mathbf{G}}$, but not by the generalized Fisher information matrix $\mathbf{G}$.

[1] B. R. Frieden, *Physics from Fisher Information: A Unification* (Cambridge University Press, Cambridge, 1998).
[2] D. Daems and G. Nicolis, Phys. Rev. E **59**, 4000 (1999).
[3] B. C. Bag, S. K. Banik, and D. S. Ray, Phys. Rev. E **64**, 026110 (2001).
[4] B. C. Bag, Phys. Rev. E **66**, 026122 (2002).
[5] D. Osorio-Gonzaler, M. Mayorga, J. Orozco, and L. R. Salazar, J. Chem. Phys. **118**, 6989 (2003).
[6] B. Q. Ai, X. J. Wang, G. T. Liu, and L. G. Liu, Phys. Rev. E **67**, 022903 (2003).
[7] G. Goswami, B. Mukherjee, and B. C. Bag, Chem. Phys. **312**, 47 (2005).
[8] S. Amari and H. Nagaoka, *Methods of Information Geometry* (AMS and Oxford University Press, Oxford, 2000).
[9] C. Tsallis, J. Stat. Phys. **52**, 479 (1988).
[10] C. Tsallis, R. S. Mendes, and A. R. Plastino, Physica A **261**, 534 (1998).
[11] C. Tsallis, Physica D **193**, 3 (2004).
[12] Lists of many applications of the nonextensive statistics are available at http://tsallis.cat.cbpf.br/biblio.htm
[13] A. Plastino and A. R. Plastino, Physica A **222**, 347 (1995).
[14] C. Tsallis and D. J. Bukman, Phys. Rev. E **54**, R2197 (1996).
[15] A. Plastino, A. R. Plastino, and H. G. Miller, Physica A **235**, 577 (1997).
[16] F. Pennini, A. R. Plastino, and A. Plastino, Physica A **258**, 446 (1998).
[17] L. Borland, F. Pennini, A. R. Plastino, and A. Plastino, Eur. Phys. J. B **12**, 285 (1999).
[18] A. R. Plastino, M. Casas, and A. Plastino, Physica A **280**, 289 (2000).
[19] S. Abe, Phys. Rev. E **68**, 031101 (2003).
[20] J. Naudts, J. Ineq. Pure Appl. Math. **5**, 102 (2004).
[21] F. Pennini and A. Plastino, Physica A **334**, 132 (2004).
[22] M. Portesi, A. Plastino, and F. Pennini, Physica A **365**, 173 (2006).
[23] M. Portesi, F. Pennini, and A. Plastino, Physica A **373**, 273 (2007).
[24] M. Masi, e-print arXiv:cond-mat/0611300.
[25] I. Csiszár, Period. Math. Hung. **2**, 191 (1972).
[26] S. Kullback, *Information Theory and Statistics* (Wiley, New

York, 1975).
[27] Hiroshi Hasegawa, Prog. Theor. Phys. Suppl. **162**, 183 (2006).
[28] A. Ohara, Phys. Lett. A **370**, 184 (2007).
[29] B. Lindner, J. García-Ojalvo, A. Neiman, and L. Schimansky-Geilíer, Phys. Rep. **392**, 321 (2004).
[30] H. Hasegawa, Physica A **374**, 585 (2007).
[31] H. Hasegawa, Phys. Rev. E **67**, 041903 (2003).
[32] H. Hasegawa, J. Phys. Soc. Jpn. **75**, 033001 (2006).
[33] H. Hasegawa, Physica A **387**, 2697 (2008).
[34] H. Sakaguchi, J. Phys. Soc. Jpn. **70**, 3247 (2001).
[35] C. Anteneodo and C. Tsallis, J. Math. Phys. **44**, 5194 (2003).
[36] H. Hasegawa, Physica A **365**, 383 (2006).
[37] K. S. Fa, Chem. Phys. **287**, 1 (2003).
[38] M. Abramowitz and I. A. Stegun, *Handbook of Mathematical Functions* (Dover, New York, 1972).
[39] H. Hasegawa, Phys. Rev. E **75**, 051904 (2007).
[40] H. Hasegawa, in *Neuronal Network Research Horizons*, edited by M. L. Weiss, (Nova Science, New York, 2007), p. 61.